Measurements of Cloud Condensation Nuclei Spectra within Maritime Cumulus Cloud Droplets: Implications for Mixing Processes

CYNTHIA H. TWOHY

National Center for Atmospheric Research, Boulder, Colorado*

JAMES G. HUDSON

Atmospheric Sciences Center, Desert Research Institute, Reno, Nevada

(Manuscript received 6 June 1994, in final form 1 October 1994)

ABSTRACT

In a cloud formed during adiabatic expansion, the droplet size distribution will be systematically related to the critical supersaturation of the cloud condensation nuclei (CCN), but this relationship can be complicated in entraining clouds. Useful information about cloud processes, such as mixing, can be obtained from direct measurements of the CCN involved in droplet nucleation. This was accomplished by interfacing two instruments for a series of flights in maritime cumulus clouds. One instrument, the counterflow virtual impactor, collected cloud droplets, and the nonvolatile residual nuclei of the droplets was then passed to a CCN spectrometer, which measured the critical supersaturation (S_c) spectrum of the droplet nuclei.

The measured S_c spectra of the droplet nuclei were compared with the S_c spectra of ambient aerosol particles in order to identify which CCN were actually incorporated into droplets and to determine when mixing processes were active at different cloud levels. The droplet nuclei nearly always exhibited lower median S_c's than the ambient aerosol, as expected since droplets nucleate preferentially on particles with lower critical supersaturations. Critical supersaturation spectra from nuclei of droplets near cloud base were similar to those predicted for cloud regions formed adiabatically, but spectra of droplet nuclei from middle cloud levels showed some evidence that mixing had occurred. Near cloud top, the greatest variation in the spectra of the droplet nuclei was observed, and nuclei with high S_c's were sometimes present even within relatively large droplets. This suggests that the extent of mixing increases with height in cumulus clouds and that inhomogeneous mixing may be important near cloud top. These promising initial results suggest improvements to the experimental technique that will permit more quantitative results in future experiments.

1. Introduction

The microphysics (droplet number concentration and size distribution) of clouds has been an important subject in atmospheric research because it influences precipitation efficiency (e.g., Albrecht 1989) and cloud albedo (e.g., Twomey 1977a). Furthermore, a fundamental understanding of cloud microphysics is necessary in order to interpret the magnitude of cloud feedback in response to global warming (Arking 1991). The microphysical properties of clouds are dependent on the characteristics of the cloud condensation nuclei (CCN) as well as a number of other factors. These relationships are discussed below.

a. Simple adiabatic growth considerations

In an updraft expanding adiabatically, cloud droplet number concentration is determined in the early stages of cloud growth when a maximum water vapor supersaturation S_m is achieved near cloud base. Maximum water vapor supersaturation occurs when the supersaturation generated by the rising and cooling of moist air is balanced by water vapor removal onto the increasing surface area of the growing droplets. After S_m, water condensation will only occur on the already existing cloud droplets. The amount of condensed water is dependent only on large-scale parameters, specifically, cloud-base temperature and lapse rate. Therefore, the droplet number concentration N_d determines how the condensate is partitioned to the droplets and affects the droplet size distribution.

Under adiabatic conditions, droplet number concentration is determined to a great extent by the available number of cloud condensation nuclei (e.g., Twomey and Squires 1959). A wide range of CCN concentrations, from several thousand per cubic centimeter (e.g., Herrera and Castro 1988) to less than

* The National Center for Atmospheric Research is sponsored by the National Science Foundation.

Corresponding author address: Dr. Cynthia H. Twohy, Research Aviation Facility, NCAR–Atmospheric Technology Division, P.O. Box 3000, Boulder, CO 80307-3000.
E-mail: twohy@ncar.ucar.edu

$10\ cm^{-3}$ (Radke and Hobbs 1969; Hindman et al. 1994), exist in the atmosphere, so droplet number concentrations can also vary considerably. Moreover, a significant but as yet unknown proportion of CCN are anthropogenic (Squires 1966; Hudson 1991; Frisbie and Hudson 1993). CCN can affect cloud albedo through their influence on droplet number and size, thus anthropogenic CCN are potentially important to global climate (e.g., Liou and Ou 1989; Charlson et al. 1992; Wigley 1991; Kaufman et al. 1991; Hudson 1993a). The size distribution of CCN may also be modified by aqueous-phase chemistry, particle scavenging, or coalescence within clouds (e.g., Hoppel et al. 1990; Bower and Choularton 1993), and these changes may alter the direct radiative impact of atmospheric aerosol particles.

CCN are characterized in terms of the critical supersaturation S_c of the particles. When a CCN grows by water vapor deposition and exceeds its critical radius, the radius at which the nucleus is in equilibrium with the atmosphere at S_c, it will continue to grow and form a fully developed cloud droplet (e.g., Mason 1971). The S_c is determined by the size and composition of the particle and is related to the number of soluble ions within a particle; larger, more soluble particles will have lower S_c values than smaller, less soluble particles (Hudson and Clarke 1992). [Organic materials could coat particle surfaces, possibly inhibiting particle growth and effectively altering their S_c; however, the type of CCN instrument used in this study has the unique capability of sensing such changes (Hudson 1993a).] Particles that have S_c values less than S_m form activated cloud droplets if given sufficient time for growth (Squires 1952), while those with higher S_c's remain as smaller unactivated droplets, or haze droplets.

In a cloud formed under adiabatic conditions, the cloud droplet concentration will equal the concentration of nuclei with $S_c < S_m$. Therefore, CCN are usually defined as those particles that have S_c's less than some maximum value. Different clouds produce different S_m depending on the updraft velocity and the CCN characteristics (Twomey 1977b). This is relevant because clouds such as cumuli experience higher updraft velocities, and therefore, have higher supersaturations than stratus clouds (e.g., Mason 1971; Hudson 1984).

It is extremely difficult to measure supersaturations in clouds, and direct observations have been limited to measurements in fog (Gerber 1991). The small amount of knowledge of cloud supersaturations has come from comparisons of the nucleating properties of ambient aerosol particles with cloud droplet number concentrations (e.g., Twomey and Squires 1959; Jiusto 1966; Twomey and Warner 1967; Warner 1969; Fitzgerald and Spyers-Duran 1973; Hudson 1980, 1983; Leaitch et al. 1986; Hegg et al. 1991). Specifically, the number of particles active at any particular supersaturation may be measured by a CCN counter, which generates this supersaturation and allows particles to grow to sizes detectable by optical means. CCN counters subject particles to the small supersaturations (<1%) found in real clouds (Squires 1972), and a CCN spectrum is produced when the number of particles that activate at several discrete supersaturations is measured.

Cloud droplets will form preferentially upon the lowest S_c nuclei (those with $S_c < S_m$). Thus, a CCN spectrum can be integrated up to the appropriate S_m in order to predict the droplet number concentration of a cloud formed adiabatically. Simple adiabatic theory also predicts that the nuclei with the lowest S_c will produce the largest droplets (e.g., Howell 1949). This can result in important differences in the chemical composition and solute concentration between droplets of different sizes (Twohy et al. 1989). The situation established by adiabatic growth, with the largest droplets containing the lowest S_c nuclei and progressively smaller droplets containing nuclei with progressively higher S_c's, will be referred to as the "adiabatic" relationship. Other cloud processes are evaluated below, primarily in terms of how they may influence this relationship.

b. *Effects of mixing*

The relatively simple relationship between the CCN spectrum and the droplet spectrum described so far applies strictly only to cloud regions established through adiabatic expansion. Such regions do occur in the atmosphere (e.g., Jensen et al. 1985) but usually comprise a relatively small fraction of cloud volume (e.g., Mason 1971). Most regions in clouds have less liquid water than would be predicted from simple upward motion and expansion of air parcels (e.g., Fletcher 1969). These subadiabatic liquid water contents can be caused by drier air being entrained from above or from the sides of the cloud or by depletion of water through precipitation.

Mixing of drier air into a cloud can also cause droplet evaporation, resulting in a reduction in the droplet number concentration. The smaller number of droplets can then grow in subsequent supersaturation cycles to sizes that are large enough to initiate coalescence (e.g., Hocking 1959; Beard and Ochs 1993). This could change the relationship between the CCN spectrum and the droplet spectrum, but the effect will vary depending on how evaporation proceeds.

Homogeneous mixing theories (i.e., Mason and Jonas 1974; Lee et al. 1980) suggest that all droplets in a mixed parcel are exposed to the same degree of subsaturation. As a result, all droplets are shifted to smaller sizes, but their sizes relative to each other remain the same. This proportional evaporation of droplets means that the smallest cloud droplets may be evaporated to haze droplets, while the larger droplets are more likely to survive. The lowest S_c particles will

still be the ones that are associated with the largest cloud droplets. Thus, the homogeneous mixing process does not change the fundamental relationship between relative droplet size and nucleus S_c that is expected for adiabatic growth.

Inhomogeneous mixing (Baker et al. 1980) has a very different effect. In this scenario, the mixing time constant is greater than the time constant for evaporation, so evaporation takes place before mixing is complete. In the extreme, this results in the evaporation of all droplets *regardless of size* within some cloud parcels, with other parcels remaining unaffected by mixing. The evaporated parcels then would contain only unactivated CCN of all S_c's, while the unaffected parcels maintain all nuclei within activated droplets. Droplet evaporation in the entity mixing scenario (Telford and Chai 1980) produces similar results (Beard and Ochs 1993).

Mixing of evaporated and unevaporated parcels with subsequent condensation is predicted to result in faster growth of large droplets in the inhomogeneous mixing case than in the homogeneous case (Baker et al. 1980). As several cycles of evaporation and supersaturation can occur within a cloud, supersaturations subsequent to the initial S_m are expected to modify the relationship between the CCN spectrum and the droplet spectrum. With successive cycles of inhomogeneous mixing, condensation and growth to large sizes is possible even on CCN with high S_c values. Consequently, there is less of an association between droplet size and S_c of the nuclei (Hudson and Rogers 1986): some particles with low S_c's may not have droplets condensed upon them, while particles with high S_c's may act as nuclei of even large droplets because they happen to survive evaporation events.

Even without entrainment, turbulent fluctuations within the cloud can cause particles to follow different trajectories, resulting in spatial variations in supersaturation and in the number of particles activated (Cooper 1989). If parcels with these different histories are mixed within the cloud or are combined during the sampling process, any relationship between the CCN spectrum and the cloud droplet size distribution will be more difficult to detect.

c. *Effects of clouds on CCN*

CCN may undergo changes in their size and composition (and consequently, S_c) due to cloud processing. Hoppel et al. (1990) examined two cloud processes that can affect the CCN spectrum that is released from a cloud: 1) trace gas (principally SO_2) absorption by droplets followed by chemical conversion to dissolved sulfate within the droplets (Easter and Hobbs 1974; Walcek and Taylor 1986; Hegg and Larson 1990) and 2) convective scavenging of interstitial particles by droplets. Hudson and Frisbie (1991) showed that droplet coalescence can also have a profound effect on both the number concentration and size of CCN.

Sulfate production, convective scavenging, and coalescence all can increase the size of the original CCN, particularly after repeated cycles of cloud formation and evaporation. Assuming the added material is soluble, the CCN affected by these processes will be shifted to lower S_c values. Since the magnitude of this effect is likely to vary with droplet size (e.g., Twohy et al. 1989; Ogren and Charlson 1992), deviations from the adiabatic relationship between droplet size and the associated CCN spectrum can result. Also, affected nuclei will activate and grow more readily in subsequent condensation cycles.

d. *Direct associations between CCN and cloud droplets*

It is apparent from the above discussion that the adiabatic relationship between CCN and cloud microphysics may be complicated by a variety of factors. Detailed cloud models have, in fact, predicted that substantial deviations can occur if mixing and chemical reactions are active (Flossmann et al. 1985; Flossmann 1991; Hegg and Hobbs 1979; Roelofs 1992). Measurements in real clouds are needed to validate these models and to understand the effects of mixing and other cloud processes on CCN–droplet relationships.

Previous experimental studies suggest that particle S_c and droplet size are, in fact, related in stratus clouds. Hudson (1984) and Hudson and Rogers (1986) compared the characteristics of interstitial cloud particles, obtained by removing cloud droplets from the sample with a cyclone separator, with the S_c spectrum of combined interstitial and droplet residual particles from fogs and mountain-impacted stratus clouds. As particles with higher S_c's were left in the interstitial sample, it was inferred that the lower S_c nuclei were present in the droplets. Also, removal of progressively larger droplets from the sample indicated that the S_c of the droplet nuclei increased with decreasing droplet size.

In experiments with a similar goal but with a different experimental approach, a counterflow virtual impactor (CVI) was used to separate droplets from interstitial particles and gases and then evaporate the droplets, allowing the residual droplet nuclei to be measured directly. The CVI essentially performs the inverse operation from the cyclone separator: droplets larger than specific sizes are included in the CVI sample, while the smaller droplets and interstitial aerosol are removed by inertial separation (Ogren et al. 1985; Noone et al. 1988b). Using this technique to sample stratiform clouds, a relationship was observed between cloud droplet size and the size of the droplet nuclei, with larger droplets containing larger nuclei (Noone et al. 1988a; Heintzenberg et al. 1989; Ogren et al. 1989; Ogren et al. 1992). Assuming that the residual nuclei were composed of primarily soluble material, cloud processes apparently did not remove the tendency of the largest droplets to be associated with the lowest S_c particles in these stratus clouds.

We present here the first direct measurements of the critical supersaturation of residual particles extracted from cloud droplets, obtained by combining the CVI with a continuous-flow CCN spectrometer (Hudson 1989). The S_c spectra of ambient particles and of residual particles from droplets were compared, and variations in the characteristics of the residual droplet nuclei with height were explored. One technical purpose of the study was simply to test the feasibility and usefulness of this technique; another scientific goal was to determine if mixing processes act to alter the adiabatic relationship between nuclei S_c and the droplet size distribution in maritime cumulus clouds. Although the CCN spectrum is known to have an impact on the microphysical development of stratocumulus clouds, the importance of CCN in the microphysics of entraining cumuli is not so well defined (e.g., Jensen and Baker 1989; Bower and Choularton 1992). In cumulus clouds, mixing can be more vigorous and can occur at many levels (Blyth et al. 1988); therefore, the effects of mixing may be more observable in cumuli than in other cloud types.

2. Experiment

a. Design

Cumulus cloud bands forming off the northeast coast of the island of Hawaii were measured during the Hawaiian Rainband Project (HaRP). A major purpose of HaRP was to investigate the dynamical and microphysical processes that force the convection and often result in intense rainfall. Twenty-nine research flights with an instrumented aircraft were conducted between 19 July and 22 August 1990 from Hilo, Hawaii. Measurements of ambient CCN were obtained from the aircraft and have been presented in detail by Hudson (1993b). For simplicity in this paper, the term *rainband* is used to refer to the cumulus cloud bands, whether or not they have developed to the rain-producing stage.

The National Center for Atmospheric Research (NCAR) Lockheed Electra was used to penetrate the rainbands at different levels and stages of development. A typical flight path that resulted in the acquisition of most of our data involved crossing the rainband, perpendicular to its axis, at several different altitudes (Fig. 1). Cloud-base altitudes were about 400–800 m and the height of the trade inversion was 1500–2500 m. Isolated turrets at cloud top often extended above the inversion. Cloud droplet size distributions were measured by a Particle Measuring Systems (PMS) forward-scattering spectrometer probe (FSSP-100) mounted on the side of the aircraft fuselage.

A counterflow virtual impactor sampled droplets during the cloud passes. Ground-based calibrations (Noone et al. 1988b) have verified that the minimum droplet size collected by the CVI can be calculated by impaction theory. The minimum droplet size sampled

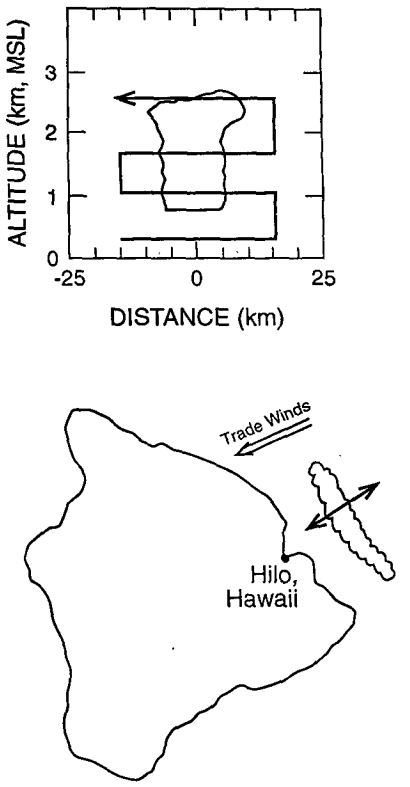

FIG. 1. Typical flight pattern used to measure rainband properties during the Hawaiian Rainband Project.

by the CVI with 50% efficiency, the "cut size", is determined by the geometry of the inlet and the aircraft speed and was about 9-μm diameter for this study. By changing the counterflow rate out through the tip of the CVI, the cut size of the instrument can be altered and the characteristics of droplets in different size ranges can be compared. The efficient rejection by the counterflow air of particles that were not associated with cloud droplets and the purity of the sample lines were verified by sampling with the CVI when *outside* of the cloud; the particle number concentration measured under these circumstances was typically less than 1 cm^{-3}.

After the droplets were separated from interstitial particles at the CVI inlet, the droplets were evaporated and the nonvolatile residual particles, termed "droplet nuclei" here, were measured by the CCN spectrometer. (Due to possible chemical reactions, coalescence, etc., these residual nuclei may not necessarily be identical to the original CCN on which the droplets formed, but later we argue that these processes do not affect our results.) The spectrometer used in HaRP has been described by Hudson (1989). This continuous flow, thermal-gradient diffusion chamber produces a CCN spectrum corresponding to a wide range of critical supersaturations (0.01%–0.8%). The CCN number concentration N discussed in this work is the total number

of particles determined by the spectrometer to have critical supersaturations of less than or equal to 0.8%.

The CVI inlet was located 6.4 m behind the aircraft radome in a center overhead mounting port, and the clear-air aerosol inlet was mounted 4.4 m behind the radome, also on the centerline. The CVI inlet extended 46 cm from the aircraft fuselage while the other inlet extended 20 cm out. The flow system that allowed the spectrometer to sample either ambient particles from the aerosol inlet (usually when outside of cloud) or droplet nuclei from the CVI inlet (usually within the cloud) is illustrated in Fig. 2. The three-way valve was used to switch from ambient air to the CVI sample line, usually just prior to cloud entry. [Measurements from the aerosol inlet were not generally reliable in cloud due to the likelihood of drop breakup, as discussed by Twohy (1992a) and Hudson (1993b)]. The diameter of particle expected to impact with 50% efficiency (Cheng and Wang 1975) in the 90° bends downstream of the CVI inlet was calculated to be about 16 μm for the 10-mm-diameter tee and about 10 μm for the three-way valve. Since most droplets would have evaporated to sizes of 1 μm or less prior to reaching the tee or valve, impaction losses in these bends should be negligible. Further details and limitations of CVI sampling characteristics are discussed in the appendix.

b. Strategy

One interesting experiment would be to examine droplet nuclei characteristics as a function of droplet size by varying the minimum cut size of the CVI. However, this would require multiple passes through the same cloud region or through an extensive, horizontally homogeneous portion of cloud. As flight tracks in HaRP seldom involved multiple passes at a single altitude, and microphysical characteristics often varied rapidly across the band, the characteristics of individual cloud parcels as a function of droplet size could not be resolved directly.

Instead, most droplet sampling was conducted at relatively large cut sizes, usually larger than the mean droplet size in the cloud. In most cases, the number of smaller droplets excluded from the CVI sample was greater than the number of larger droplets excluded by inefficient transmission (appendix), and the sample was weighted toward the large-droplet end of the size distribution. The S_c spectra of nuclei within these relatively large droplets at different cloud levels were then compared to ambient below-cloud CCN spectra, with potential implications for mixing processes as discussed below. A few samples of droplet nuclei from cloud-base regions were also taken at relatively small cut sizes that encompassed most of the droplet size distribution.

Some simulated examples of the effects mixing may have on the S_c spectrum of droplet nuclei are displayed in Figs. 3 and 4; these plots are also used later for comparison with our data. In each panel, the critical supersaturation (in percent) is plotted on the abscissa, and the cumulative percent of the total ambient CCN spectrum activating at various S_c's is on the ordinate. Figure 3a shows a typical below-cloud CCN spectrum (dashed line) as well as the S_c spectrum of droplet nuclei (solid line) when half the total available particles have

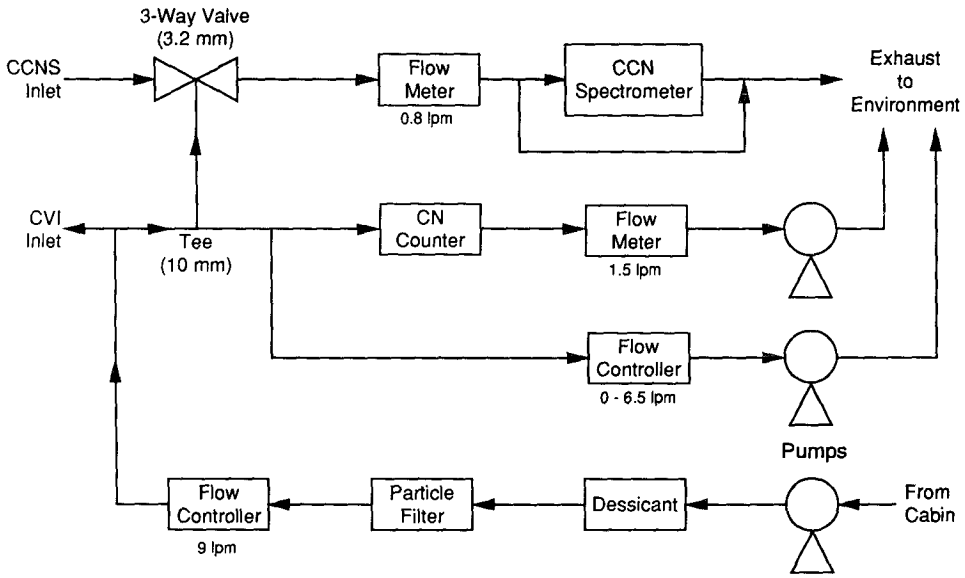

FIG. 2. Flow system used during HaRP to link the CVI and CCN spectrometer. The CVI system has been simplified for clarity (arrow pointing outward at location of CVI inlet signifies the counterflow air, which is used to exclude interstitial particles and gases). The bypass line around the CCN spectrometer serves to prevent diffusional loss of particles upstream of the instrument. Numbers below the three-way valve and tee on the left side of the figure refer to the orifice diameter. Flow rates are also given in liters per minute.

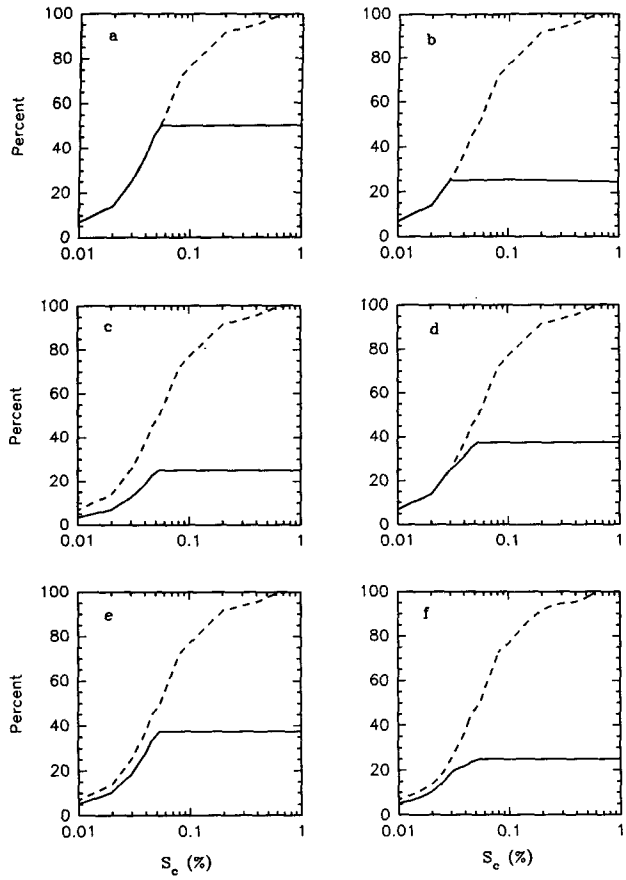

FIG. 3. Examples of the types of S_c spectra expected within droplets in a cloud undergoing different mixing processes. In all plots, the percent critical supersaturation is plotted on the abscissa and the cumulative percent of total particle number on the ordinate. Dashed lines represent a typical below-cloud CCN spectrum, and solid lines represent the simulated S_c spectrum of droplet nuclei in parcels under the following conditions: (a) adiabatic growth, 50% of particles activated; (b) homogeneous evaporation of 50% of droplets in adiabatically formed parcel a; (c) inhomogeneous evaporation of 50% of droplets in parcel a; (d) 1:1 mixture of adiabatically formed parcel a and homogeneously evaporated parcel b; (e) 1:1 mixture of adiabatically formed parcel a and inhomogeneously evaporated parcel c; and (f) 1:1 mixture of homogeneously evaporated parcel b and inhomogeneously evaporated parcel c.

been activated in an adiabatic ascent. In this case, particles that activate at supersaturations less than or equal to about 0.05% are incorporated into the droplets, but the supersaturation achieved by the hypothetical cloud is insufficient to activate the remaining particles. Therefore, the solid and dashed lines are congruent up to about 0.05% S_c, but at higher S_c's the solid line representing the droplet nuclei is horizontal since no particles with higher S_c's are activated.

Homogeneous evaporation is essentially the converse process of adiabatic growth, and the effect of homogeneous mixing on this same parcel would be to evaporate the smaller droplets with nuclei S_c's between about 0.03% and 0.05% (Fig. 3b). The remaining larger droplets would retain the lower-S_c nuclei, and the adiabatic relationship would be preserved—the lower-S_c particles are present within droplets, and of the droplet nuclei, those with the lowest S_c's comprise the nuclei of the largest droplets. Inhomogeneous or entity mixing, on the other hand, could act to evaporate all droplets in one parcel, while evaporating none in another. This would result in an apparent evaporation of 50% of the droplets in the parcel formed adiabatically (plot a), *independent of droplet size,* for the ensuing mixed parcel (Fig. 3c).

Other possible scenarios that may result from subsequent combination of various cloudy parcels are as follows: Fig. 3d—a combination of the homogeneously mixed parcel (plot b) and the adiabatically formed parcel (plot a); Fig. 3e—a combination of an inhomogeneously mixed parcel (plot c) and the adiabatically formed parcel (plot a); or Fig. 3f—a homogeneous (plot b)-inhomogeneous (plot c) mixture. These last three cases will be referred to as "in-cloud" mixing in order to distinguish them from the mixing of clear air and cloudy air considered earlier. All these scenarios are depicted in order to show the range of spectral shapes that can occur in real clouds, either through mixing with subsaturated air from outside cloud, in-cloud mixing of parcels with different histories, or even mixing of different parcels during the actual airborne sampling process.

In Fig. 4, the six scenarios shown in Fig. 3 are depicted in the same sequence, except a higher maximum supersaturation is assumed in Fig. 4 so that 100% of the particles are activated in the parcel during adiabatic expansion (Fig. 4a). Note that this initial activation of even the high-S_c particles means that some of these particles can remain in droplets in all mixing scenarios except for that of simple homogeneous mixing (Fig. 4b). The distribution of nuclei S_c with droplet size varies with the mixing type, however, as discussed below.

The measured characteristics of the nuclei from cloud droplets can be compared with the curves in Figs. 3 and 4 to provide insight into the mixing processes active in a particular cloud region. Although all of the mixing processes exhibit a deviation of the droplet nuclei curve below the ambient particle curve at higher S_c's, only pure homogeneous mixing (Figs. 3b and 4b) exactly follows the ambient spectrum at low S_c's and then abruptly levels off. Parcels that have undergone homogeneous mixing become less easy to distinguish, however, when they are mixed with adiabatically formed parcels (Figs. 3d and 4d) or with inhomogeneously mixed parcels (Figs. 3f and 4f).

The ability to separate and examine the characteristics of only the larger droplets becomes useful in identifying when inhomogeneous mixing is a dominant process. In particular, inhomogeneous mixing is indicated if the larger droplets contain some of the highest-S_c particles, using the following reasoning: in the homogeneous mixing case, no droplets contain the

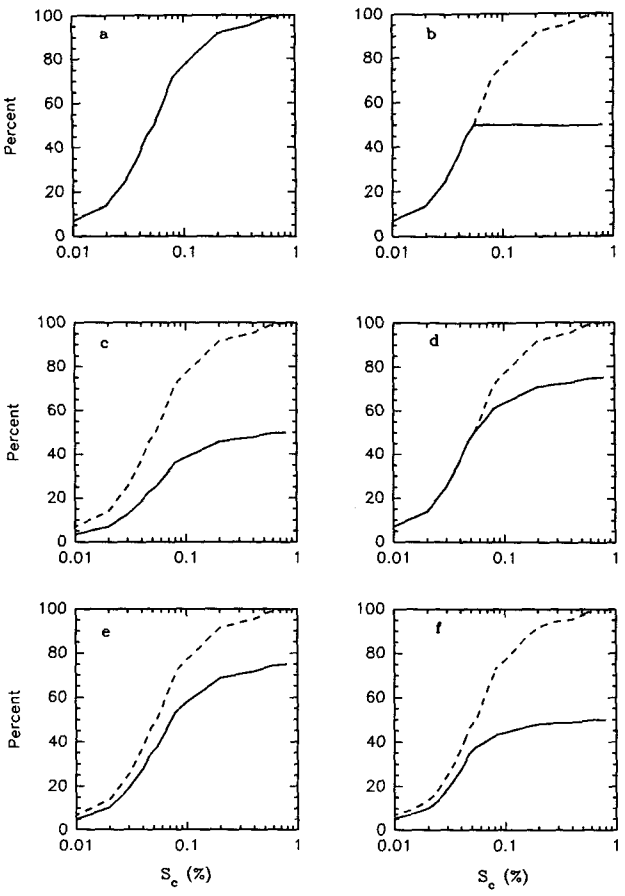

FIG. 4. Same as Fig. 3 but with 100% of particles activated in adiabatically formed parcel (higher maximum supersaturation).

highest-S_c nuclei because all the small droplets that originally contained these particles have evaporated. Figure 4e, a mixture of homogeneously evaporated and adiabatic-formed parcels, reflects the involvement of high-S_c nuclei; however, these are present only in the smallest droplets that were originally present in the adiabatically formed cloud region. In contrast, with large initial supersaturations and subsequent inhomogeneous mixing (Fig. 4c), some droplets originally of all sizes (and having nuclei with various S_c's) survive the evaporation process. With many cycles of evaporation and subsequent condensation, these droplets can ultimately grow to the largest droplet sizes.

Subsequent supersaturations could occur with any of the above scenarios, one effect of which could possibly be to activate more particles. These might originate from the entrained air, or in the case of inhomogeneous mixing, from regions originally containing droplets that were subsequently completely evaporated. These particles will tend to form droplets that are small relative to those surviving the previous evaporation, yet their S_c could be large. Characteristics of nuclei from the entire droplet spectrum could therefore become more complex, but the S_c characteristics of the larger droplets would still be preserved.

Coalescence, aqueous-phase oxidation of SO_2, and scavenging of particles or trace gases can potentially lower the S_c of a droplet's residual nucleus by adding soluble material to it. We do not believe that these processes significantly influence our results for the following reasons. First, nuclei from droplets larger than 40 μm are not transmitted by the CVI (see appendix), so few droplets that had undergone coalescence were included in the CVI samples (e.g., Pruppacher and Klett 1978). Cloud regions containing drizzle and precipitation were also eliminated from the dataset because of the drop breakup phenomenon discussed in the appendix. Aqueous chemistry and scavenging effects are discussed below.

We cannot completely rule out the possibility that some enhancement of the droplet nuclei size could have occurred due to aqueous-phase sulfate production, as modeling studies (e.g., Bower and Choularton 1993) and measurements (Hoppel et al. 1990) suggest that significant sulfate may be produced under certain conditions. We expect this process to have little, if any, effect on our results for the following reasons. First, the CCN in the marine environment are likely to be composed of acidic NH_4HSO_4 or H_2SO_4 (e.g., Huebert and Lazrus 1980; Clarke et al. 1987), and droplet acidity resulting from nucleation scavenging will limit the amount of sulfate produced. [Cloud water pH in this location has previously been measured to be low (Parungo et al. 1982).] Also, concentrations of gaseous SO_2 (the precursor of sulfate produced in the aqueous phase) are usually below the instrumental detection limit (200 pptv) in nonvolcanically influenced boundary layer air measured at Mauna Loa Observatory (G. Hübler 1994, personal communication). Finally, the aforementioned studies predict that the primary impact of sulfate production should be on nuclei of the smallest cloud droplets, as they have a relatively small CCN mass and a higher pH (neglecting coarse-mode sea-salt particles, which are relatively few in number and inefficiently sampled). Our analysis focuses mainly on the larger cloud droplets.

Regarding particle scavenging, substantial soluble mass would have to be added to droplets to noticeably decrease S_c values, but scavenging of sizeable aerosol particles is relatively slow for the conditions in which we measured. For example, although the scavenging half-life of 0.01-μm-radius particles is only about 1 h [using Eq. (12-92) of Pruppacher and Klett (1978), with a mean droplet radius of 10 μm and a liquid water content of 1 g m^{-3}], the scavenging half-life of 0.1-μm-radius particles is about 60 h. Also, the number of particles available to be scavenged is low in the unpolluted environment. [An insoluble particle, if incorporated into a droplet by scavenging, could produce an additional residual nucleus after droplet evaporation, but the majority of particles in the Pacific marine

environment are soluble sulfate compounds (e.g., Clarke et al. 1987).]

For these reasons, we believe that adiabatic expansion and mixing processes were the primary factors governing the relationship between S_c of the droplet nuclei and droplet microphysics in our experiment.

c. *Analysis*

Several steps were taken to put the data into the form that is presented here. First, as discussed in the appendix, time periods when large drop breakup occurred inside the CVI were eliminated from the dataset. Next, data from the CCN spectrometer needed to be synchronized with the other instruments because the CCN response lagged by 30–50 s, depending upon the flow rate to the spectrometer. The time interval between maxima in the FSSP number concentration when passing through cloud and maxima in the number of droplet nuclei measured by the spectrometer was used as the effective lag time of the CCN instrument for each flow rate. Determination of this lag time was limited by the integration period (2–10 s) of the CCN samples. Some uncertainty is therefore introduced in comparisons between the CCN spectra of droplet nuclei and the measured microphysical cloud properties by mismatches in the beginning and/or end times of the sample periods. Sequential CCN samples that exhibited similar number concentrations and spectral shapes were averaged to reduce these temporal uncertainties.

The median S_c (on the basis of number concentration) was used as a characteristic statistic to summarize the spectra of both ambient particles and droplet nuclei. Median S_c's were rounded to the nearest 0.01% S_c. This represents several channels of the optical particle counter used with the CCN spectrometer for S_c's less than 0.10%, so differences in median S_c's $\geq$ 0.01% should be considered significant for these low S_c's. For median S_c's greater than 0.10%, the uncertainty in the measured spectra is larger than the rounding error and is estimated to be $\pm$0.02% S_c. Future references to $\bar{S}_c$ refer to the median S_c.

3. Results

a. *Overall data summary*

Table 1 contrasts the median S_c of ambient CCN and droplet nuclei measured by the CCN spectrometer during several HaRP flights. Each row in the table lists the time and altitude range over which an individual cloud band was sampled; also given are the average of $\bar{S}_c$ values obtained for ambient aerosol samples in the environment surrounding the band ("ambient" column) and for horizontal passes through the band ("droplet nuclei" column). The table includes all usable in-cloud data (i.e., when droplet breakup did not occur) for bands where at least two samples were obtained. Cumulative distances encompassed within each sample ranged from 600 m to 10 km, with sampling times governed by the cloud extent and its microphysical variability. The purpose of Table 1 is simply to summarize the data and convey the overall sense of the results. Since these data were obtained from a variety of cloud regions in different stages of development, more detailed information will be examined later for several cases.

TABLE 1. Average $\bar{S}_c$ of CCN spectra. Each time period corresponds to one cloud or cloud band. The number of samples averaged is given in parentheses.

Date 1990	Time (UTC)	Altitude (m)	Ambient $\bar{S}_c$ (%)	Droplet nuclei $\bar{S}_c$ (%)
2 Aug	1758–1820	900–1900	0.14 (5)	0.02 (6)
2 Aug	1820–1912	300–2000	0.15 (4)	0.08 (12)
3 Aug	1744–1823	1500–2300	0.39 (3)	0.33 (9)
5 Aug	0223–0257	600–1400	0.34 (6)	0.27 (8)
5 Aug	0241–0256	700–1100	0.32 (4)	0.24 (6)
5 Aug	0300–0323	100–1500	0.26 (3)	0.15 (3)
5 Aug	0412–0430	400–1300	0.25 (2)	0.22 (4)
8 Aug	0928–1022	200–1600	0.05 (10)	0.03 (7)
8 Aug	1039–1135	500–2700	0.14 (4)	0.05 (9)
10 Aug	1800–1901	1100–2700	0.25 (7)	0.08 (4)
10 Aug	1908–1930	800–1900	0.14 (4)	0.02 (2)
10 Aug	1930–1945	1100–2100	0.12 (4)	0.11 (7)
20 Aug	1832–1854	500–1100	0.27 (4)	0.20 (6)
20 Aug	1912–1937	1000–1600	0.32 (4)	0.19 (5)
20 Aug	1950–1958	500–1400	0.30 (2)	0.16 (4)

In examining Table 1, it is apparent that the $\bar{S}_c$'s of the ambient CCN samples varied considerably throughout the project. These variations in $\bar{S}_c$ could be a result of collision-coalescence processes, with different efficiencies of CCN removal through precipitation. If coalesced drops had evaporated before reaching the ground, for example, the released CCN would be enlarged and the measured $\bar{S}_c$ would be relatively low; if, however, the coalesced drops were all removed as precipitation to the ocean surface, lower-S_c particles would be preferentially removed and the measured $\bar{S}_c$ could be relatively high.

The number concentration and $\bar{S}_c$ of the ambient particles sometimes increased with height (Hudson 1993b). In a previous study of Hawaiian rainbands, Raga et al. (1990) concluded that while entrainment occurred extensively at the sides of the cloud bands, approximately 7% of the air cycled through the cloud had originated above the inversion, where downdrafts were generated by either evaporative cooling or mechanical forcing. CCN within droplets near entraining regions at the edges or top of the cloud may therefore be a mixture of CCN from below cloud base and from other clear air regions around the cloud. The source region of droplet nuclei will depend on a variety of factors including the cloud age, the vapor deficit in the entrained air, the pressure scale of the entrainment, and the droplet size (Baker and Latham 1992). The below-cloud CCN spectrum is not, therefore, neces-

sarily representative of the CCN spectrum on which all droplets formed. Also, coalescence and precipitation can modify the below-cloud aerosol spectrum throughout the cloud's life cycle, as discussed earlier.

Table 1 indicates that when $\bar{S}_c$'s were averaged across the band, droplet nuclei always exhibited a lower $\bar{S}_c$ than CCN sampled below the cloud or around the cloud at similar altitudes. Particles with higher S_c's were therefore not incorporated into droplets sampled by the CVI as frequently as particles with lower S_c's. However, our observations are not necessarily inconsistent with the notion that some nuclei with high S_c formed droplets; in fact, particles with relatively high S_c's were occasionally present even in samples from only the large end of the droplet size distribution. Also, individual samples of droplet nuclei from near cloud top occasionally exhibited $\bar{S}_c$'s that were quite high.

The table also suggests that the magnitude of the differences between ambient and droplet nuclei $\bar{S}_c$'s varied for the different cloud bands. This was not necessarily due to differences in the way that particles formed droplets but could be related to the portion of the droplet spectrum sampled by the CVI; both the droplet size distributions and the CVI cut sizes differed for each band. Also, the location and number of samples that were collected varied from band to band. It is therefore informative to evaluate the characteristics of ambient particles and droplet nuclei on a case-by-case basis, as well as examining the summary statistics in Table 1.

b. *Case studies*

Three cloud bands were selected for more-detailed analysis. The first two were developing rainbands with little precipitation, one sampled near midnight on 8 August 1990 and one in the daytime on 2 August 1990. For the third case on 10 August, we focus on data from the tops of more mature, precipitating rainbands. All three bands were located approximately 25 km east of Hilo, Hawaii.

1) Case of 8 August 1990

This rainband, sampled at night (0928–1022 UTC), was in the early stages of development. Consequently, we were able to obtain samples at several levels, including just above cloud base, without encountering precipitation. Updrafts were moderate (up to 3 m s^{-1}) and droplet concentrations measured by the FSSP were up to 300 cm^{-3} in the regions of maximum updraft velocity.

The median S_c's of the ambient (solid circles) and droplet nuclei (hollow circles) spectra are plotted versus altitude in Fig. 5. As expected and as in Table 1, the droplet nuclei generally exhibit lower $\bar{S}_c$'s than the ambient CCN. The two droplet nuclei samples with $\bar{S}_c$'s of 0.04% were taken at the minimum CVI cut size of about 9-μm diameter; the other samples with lower $\bar{S}_c$'s were taken at larger CVI cut sizes ranging from 16 to 27 μm in diameter. CVI samples that included droplets over a wider size range (using lower minimum cut sizes) therefore have similar $\bar{S}_c$'s to the ambient spectra, as expected if most particles have been activated. Samples that consisted of only the larger droplets (high cut sizes) tended to lower $\bar{S}_c$'s, generally consistent with adiabatic growth or homogeneous mixing. The droplet size distributions were not the same for all samples, however, and the detailed characteristics of the measured spectra are not apparent from the median S_c alone. We present below the droplet distributions for several of the sampled cloud regions and compare the shape of the ambient and droplet nuclei S_c spectra in the context of the mixing scenarios described earlier.

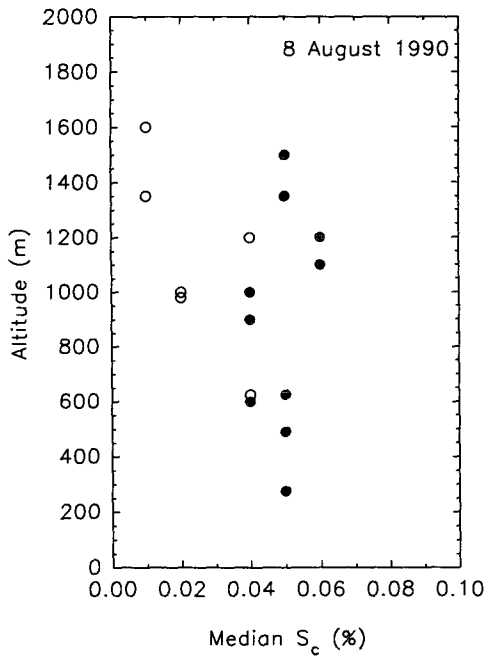

FIG. 5. Median critical supersaturation $\bar{S}_c$ of ambient CCN (solid circles) and cloud droplet nuclei (open circles) as a function of pressure altitude for cloud band sampled at 0928–1022 UTC 8 August 1990.

Droplet size distributions measured by the FSSP during three different cloud penetrations are shown in Fig. 6. The manufacturer's standard calibration was used for the FSSP sizing, rather than the sizes corrected for electronic limitations of the probe at aircraft speeds (e.g., Baumgardner and Spowart 1990). For this experiment, such corrections tended to predict droplets so large that liquid water contents were unrealistic (up to several times the adiabatic value). The reason for this is unclear, but as a consequence the root-sum-square uncertainty in the FSSP sizing may be as large as 41% (from Baumgardner et al. 1990; assuming coincidence corrections need not be applied for these low droplet concentrations). Most of this uncertainty is

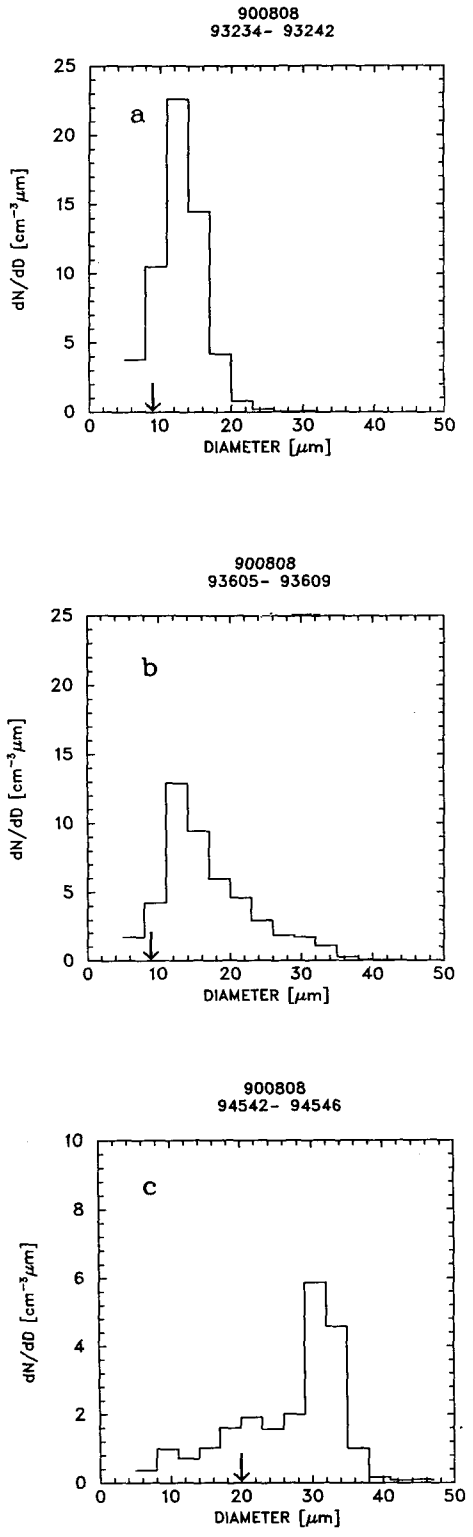

FIG. 6. Average droplet size distributions measured by the FSSP for three cloud regions sampled on 8 August 1990. Integrated number concentrations were 170 cm^{-3} for distribution (a) (625-m altitude), 141 cm^{-3} for distribution (b) (1200 m), and 66 cm^{-3} for distribution (c) (1000 m). The minimum cut size used to sample each region with the CVI is indicated by an arrow on the abscissa of each plot.

due to instrument bias, rather than precision error, so the relative differences in measured droplet size distributions should still be significant.

The distribution in Fig. 6a was measured at 625-m altitude, just above cloud base, in a region where the liquid water content was approximately adiabatic (as measured by a hot-wire probe, as well as derived from the FSSP data). The narrowness of the distribution is also typical of adiabatic growth, with few droplets larger than 20 μm in diameter. The second distribution (Fig. 6b), measured at an altitude of 1200 m, peaks at approximately the same size as the cloud-base distribution. The spectrum has widened, however, with substantial numbers of droplets between 20 and 35 μm in diameter. The final distribution (Fig. 6c) was measured at 1000 m but shows reduced droplet number concentrations (66 cm^{-3} vs 141 and 170 cm^{-3}) and significant spectral broadening indicative of mixing and subsequent condensation. The second and third regions both had liquid water contents less than the adiabatic values, suggesting that some drier air had been entrained.

The S_c spectra of cloud droplet nuclei for these three cloud regions are compared to an ambient CCN spectrum measured near cloud base (at 625 m) in Fig. 7. The comparisons were made by first scaling the measured ambient spectrum (solid circles) so that the total particle number concentration was equal to 100%. The corresponding percent of droplet nuclei at each S_c (hollow triangles) was then calculated by normalizing the number concentration of droplet nuclei activating at an S_c of 0.01% to the percentage of ambient particles activating at 0.01%. By forcing the percentages to be equal at 0.01%, we are not necessarily concluding that all of the available CCN with $S_c \leq 0.01\%$ are present in the sampled droplets; this technique was merely used to create spectral *shapes* for the ambient CCN and droplet nuclei that could be compared with those expected for different types of mixing (Figs. 3 and 4).

Absolute number concentrations are not presented in Fig. 7 as the droplet nuclei concentrations do not compare directly with the ambient particle concentrations for several reasons. First, droplet numbers are initially enhanced inside the CVI, but then some will be lost to surfaces within the CVI. Although the enhancement effect is well understood, transmission efficiency decreases with increasing droplet size and is more difficult to quantify (see appendix). The second difficulty in specifying absolute concentrations arises from the fact that the sampling period often included both cloudy and clear-air regions—although no additional particles were introduced into the sample in the clear-air regions, the average number concentration measured by the CCN spectrometer for the entire sample was reduced because of these regions. Finally, a possible problem with the CCN flowmeter on some flights meant that the absolute magnitude of the concentrations was possibly in error. The only one of these difficulties that could

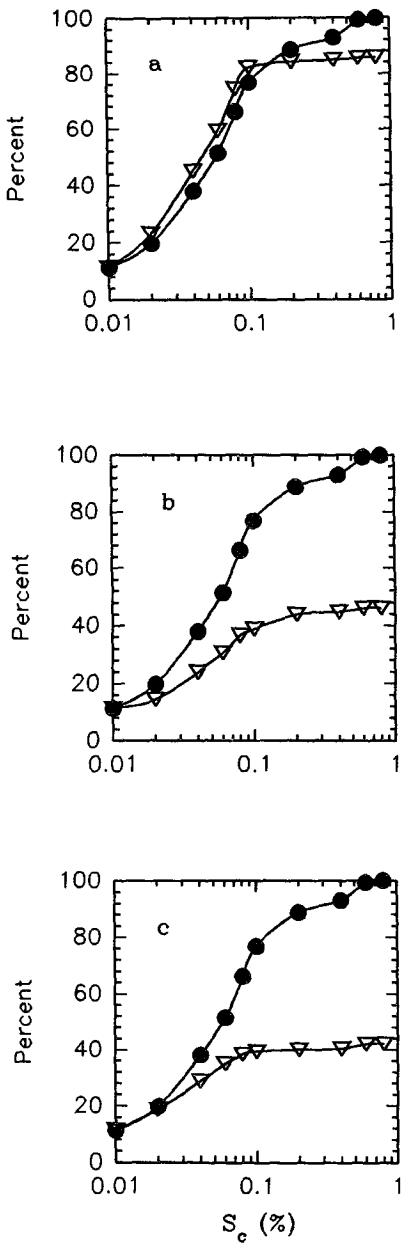

FIG. 7. CCN spectrum measured near cloud base (solid circles) and droplet nuclei spectra (open triangles) measured in three cloud regions on 8 August 1990 with droplet distributions shown in Fig. 6. Percent critical supersaturation is plotted on the abscissa and cumulative percent of total particle number on the ordinate. Distribution (a) was sampled at a CVI cut size of 9-μm diameter and had a median S_c of 0.04%. Distribution (b) was sampled at a CVI cut size of 9-μm diameter and had a median S_c of 0.04%. Distribution (c) was sampled at CVI cut size of 20-μm diameter and had a median S_c of 0.03%.

bias the *shape* of the spectra in Fig. 7 is the CVI transmission efficiency. As droplets of different sizes may be transmitted with varying efficiencies, the residual nuclei spectrum could be affected. This effect was minimized by presenting data primarily when the majority of droplets sampled had sizes near the CVI cut size, where transmission efficiency is maximized and varies slowly with droplet size (T. L. Anderson 1994, personal communication). Potential biases for specific cloud regions are also discussed below.

The spectral shape of the nuclei from droplets in the cloud-base region (Fig. 6a) with an adiabatic liquid water content is shown in Fig. 7a. Here, the CVI cut size was set at about 9-μm diameter, so most droplet sizes were sampled. The droplet nuclei spectrum has a very similar shape to the ambient spectrum up to about 0.1% S_c, at which point it flattens out. This behavior agrees with what is expected for adiabatic growth (Fig. 3a). The small upward offset of the droplet nuclei spectrum relative to the ambient spectrum below 0.1% S_c could be due to small differences (less than a few per cubic centimeter) between the number concentration of the ambient spectrum at 0.01% S_c and the spectrum on which the cloud parcel actually nucleated. We believe this is within the uncertainty of the technique and does not indicate any significant departure from adiabatic growth. Another cloud-base sample exhibited a very similar spectral shape.

The spectra of the droplet nuclei sampled in the regions with subadiabatic liquid water contents at 1200 m (Figs. 6b and 7b) and 1000 m (Figs. 6c and 7c) have a different shape from either the ambient spectrum or the spectrum of droplet nuclei in the cloud-base region. Droplets 9 μm and larger were collected for the 1200-m sample and 20 μm and larger for the 1000-m sample, encompassing most of the droplet distribution in both cases. Comparing Figs. 7b,c with Figs. 3b,c, the shape of the two samples taken at higher levels in the cloud may indicate some degree of inhomogeneous mixing (Fig. 3c) as opposed to homogeneous mixing. However, it is also possible to obtain spectral shapes similar to those in Figs. 7b,c through in-cloud mixing processes (e.g., Figs. 3d–f). Despite the apparent mixing, the lower-S_c particles were still preferentially incorporated into the cloud droplets and all three spectra flatten out at an S_c of about 0.1%.

Samples taken in the cloud regions shown in Figs. 6b,c, with relatively high concentrations of droplets much larger than the CVI cut size, might be affected by the reduced transmission efficiency of the CVI for larger droplets. Assuming that any large droplets that were not transmitted efficiently had higher percentages of low-S_c nuclei than the smaller droplets had, this could mean that lower-S_c nuclei might be underrepresented in the nuclei spectra shown in Figs. 7b,c. Greater numbers of low-S_c nuclei would only act to reduce the slope of the droplet nuclei curves further, however, with mixing still being indicated.

2) CASE OF 2 AUGUST 1990

The cloud band sampled on the morning of 2 August (1820–1912 UTC) was recently formed and moder-

ately vigorous, with maximum updraft velocities of 4 m s^{-1}. Maximum droplet concentrations were about 300 cm^{-3}, but the cloud was nonuniform with an uneven cloud base and large variations in droplet number concentrations at all altitudes.

The median S_c's measured at different levels for the ambient samples and for the droplet nuclei are shown for the 2 August case in Fig. 8. In general, the droplet nuclei exhibit lower $\bar{S}_c$'s than the ambient particles at similar altitudes. Also, there is an increase in $\bar{S}_c$ with height for both ambient particles and droplet nuclei.

The CVI minimum cut sizes were 10 μm for the cloud-base sample (725 m), 14–19 μm for the cloud-middle samples (1025–1475 m), and 22 μm for the samples at cloud top (1625–1775 m). This was an attempt to sample a similar portion of the droplet spectrum despite the growth to larger droplet sizes with increasing height, although the nonuniformity of the clouds meant that this was not always accomplished.

Figure 9 shows droplet distributions measured by the FSSP for a region near cloud base (Fig. 9a), a region at a middle cloud level of 1350 m (Fig. 9b), and a cumulus turret at 1625 m (Fig. 9c) that penetrated the base of the inversion. The cloud-base distribution exhibits a narrow range of small droplet sizes. The average liquid water content of 0.18 g m^{-3} was subadiabatic but varied from less than 0.1 to 0.32 g m^{-3} (near adiabatic). The droplet distribution taken along the cloud edge at 1350 m peaks at about the same size as the cloud-base sample but is extended at the large droplet end. Liquid water content for this region was definitely subadiabatic. Larger droplets predominate in the turret at cloud top, although the distribution is fairly wide and apparently has a second mode characterized by droplets smaller than 10 μm in diameter. Liquid water content was slightly subadiabatic in this region.

The S_c spectra of the droplet nuclei for these cloud regions are normalized and compared to an ambient below-cloud spectrum in Fig. 10. (Critical supersaturation measurements below 0.02% were not available for this flight, so droplet nuclei number percentages were normalized to the ambient spectrum at 0.02% S_c rather than 0.01% S_c as in Fig. 7.) Since the cloud-base sample was taken at a 10-μm cut size, droplets of most sizes were collected by the CVI. The cloud-base droplet nuclei spectrum is similar to the ambient spectrum up to about 0.06% S_c, then deviates below the ambient spectrum and flattens out at S_c's greater than 0.1% (Fig. 10a). This behavior is similar to that predicted if an adiabatically formed cloud region was combined with a region that had undergone homogeneous mixing, such as that shown in Fig. 3d. The characteristics of a single sample averaged across different cloud regions would not be readily distinguishable from actual in-cloud mixing of such regions; in fact, the inhomogeneity observed in droplet concentration and liquid water content across the sampled region suggests that

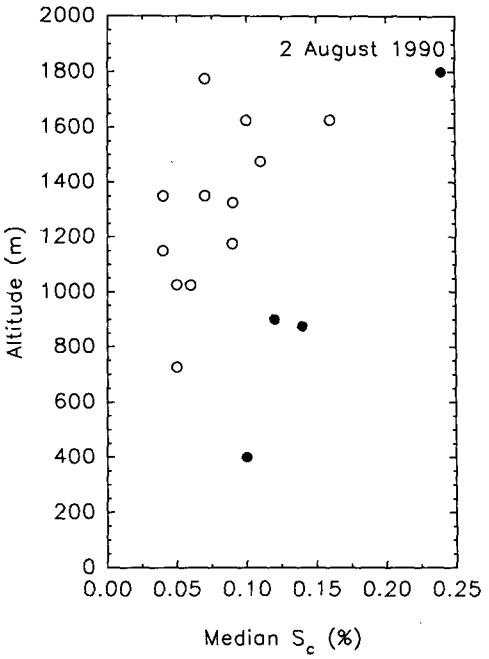

FIG. 8. As in Fig. 5 but for a rainband sampled at 1820–1912 UTC 2 August 1990.

sample averaging, rather than in-cloud mixing, could be the cause of the spectral shape in Fig. 10a.

The droplet nuclei spectrum measured for droplets larger than 19 μm at 1350 m is compared with the below-cloud spectrum in Fig. 10b. Note from Fig. 9b that only the large end of the droplet distribution was sampled in this case. The shape of the nuclei spectrum suggests some degree of inhomogeneous mixing (Fig. 3c), but again it is possible that the other in-cloud mixing processes shown in Fig. 3 could produce a similar spectrum. Nearly all the nuclei of these large droplets still have S_c's less than about 0.1%.

All three samples from the upper levels (Fig. 8) were taken in cumulus turrets, with droplets larger than 22 μm and approximately the same portion of the droplet size distribution sampled in all three turrets. However, the $\bar{S}_c$'s of the sampled turrets are substantially different. Two of the three turrets have $\bar{S}_c$ values similar to those at cloud middle and the other has an $\bar{S}_c$ of 0.16%, which is between the medians of the ambient distributions below cloud (0.10%) and above the inversion (0.24%). The final droplet nuclei spectrum shown in Fig. 10c represents this extreme situation, with the largest $\bar{S}_c$ (0.16%) of the three cloud-top samples. Even with a 22-μm cut size, a substantial portion of the droplet spectrum was sampled in this region (refer to Fig. 9c). The turret exhibits significant deviation below the curve of the ambient spectrum and approximately half of the sampled droplets have nuclei S_c's greater than 0.1%. This suggests inhomogeneous mixing may have been active in this turret. However, since the 22-μm cut size

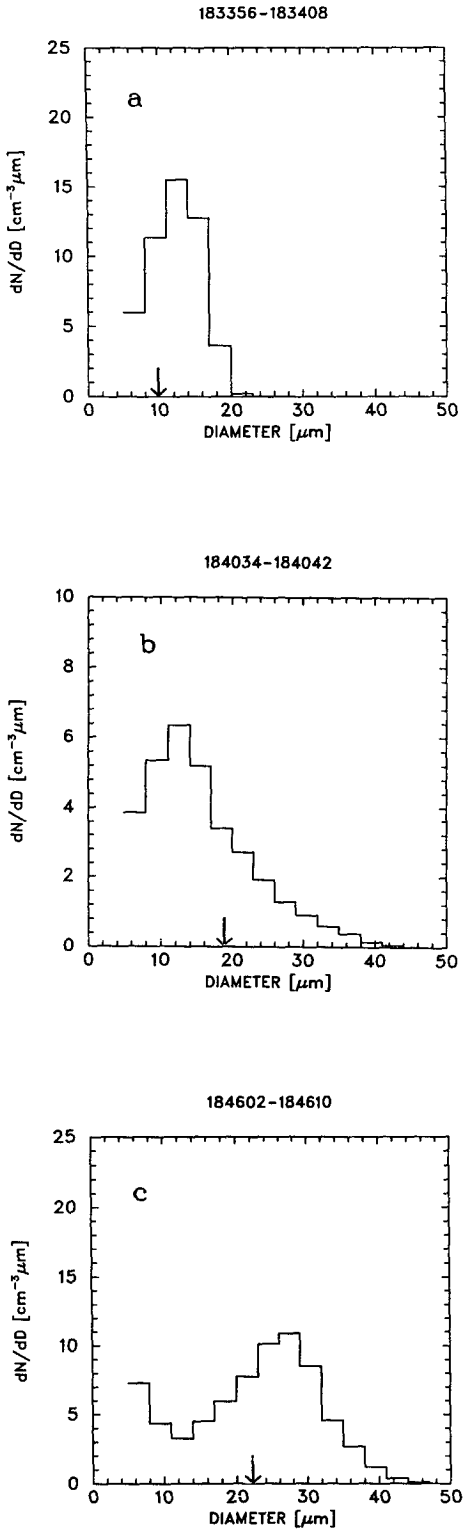

FIG. 9. Average droplet size distributions measured by the FSSP for three cloud regions sampled on 2 August 1990. Integrated number concentrations were 148 cm^{-3} for distribution (a) (725-m altitude), 96 cm^{-3} for distribution (b) (1350 m), and 208 cm^{-3} for distribution (c) (1625 m). The minimum cut size used to sample each region with the CVI is indicated by an arrow on the abscissa of each plot.

included a relatively large portion of this particular droplet distribution, and median S_c's of the ambient spectra increased with altitude on this day, it is possible that some of the high-S_c nuclei actually originated from air entrained at higher levels. In the next case, however, we observed similar behavior at cloud top even when the smaller droplets were excluded and the ambient spectra did not vary substantially with height.

3) CASE OF 10 AUGUST 1990

The cloud band sampled at 1800–1901 UTC 10 August 1990 was a fully developed, vigorous rainband with maximum updrafts of 6 m s^{-1} and precipitation-sized drops at lower cloud levels and below cloud base. As discussed earlier, data from regions of the cloud that actually contained precipitation could not be used, so usable data from lower cloud regions were scarce. Droplet number concentrations varied substantially, although mean droplet concentrations for samples in the middle and upper regions of the cloud were often quite low (<50 cm^{-3}). These low droplet concentrations at the higher cloud levels are indicative of mixing with drier environmental air, and, possibly, the effect of collision coalescence with subsequent precipitation.

Figure 11 shows the median S_c's of the ambient and droplet nuclei samples at different altitudes. The $\bar{S}_c$'s of ambient CCN vary, but not systematically with height as in the 2 August case. All droplet nuclei samples except that at 1200 m were taken at a large CVI cut size of 28-μm diameter. The droplet nuclei in the middle levels have $\bar{S}_c$'s noticeably lower than those of the ambient samples and the cloud-top samples. Like the previous case, the CVI samples taken near cloud top exhibit a substantial spread in $\bar{S}_c$. However, the above-cloud CCN spectra do not have substantially higher $\bar{S}_c$'s than spectra measured at lower altitudes.

The droplet distributions for the selected cloud regions on this day are shown in Fig. 12. The distributions in Figs. 12a,b, from the middle cloud levels (1875 and 1800 m, respectively), are similar, while the one from cloud top (2150 m) is shifted to smaller droplet sizes with a lower total number concentration (22 cm^{-3} vs 102 and 98 cm^{-3}). The first two regions had liquid water contents that were approximately half of the adiabatic value, but the liquid water content for the cloud-top region was only about one-tenth of the adiabatic value.

The measured S_c spectra corresponding to these cloud regions are shown in Fig. 13. The droplet distributions (Figs. 12a,b), cloud levels, and CVI cut sizes were approximately the same for the first two regions. The second region (Fig. 13b), however, has a higher $\bar{S}_c$ (0.06% vs 0.02%) and exhibits significant involvement of high-S_c nuclei in the droplets, even though only droplets greater than 28-μm diameter were sampled. The last plot (Fig. 13c) shows the cloud-top case with the highest $\bar{S}_c$ (0.23%). Here, even nuclei with

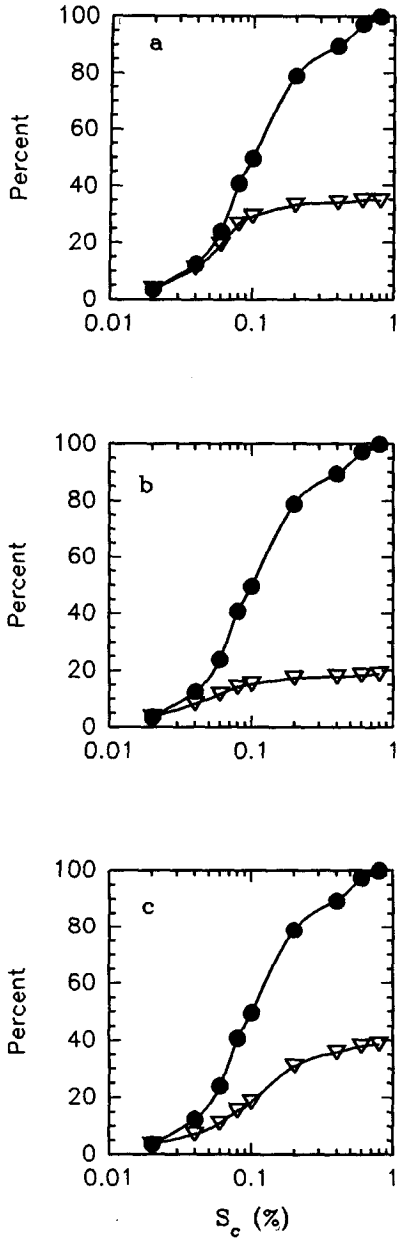

FIG. 10. Below-cloud CCN spectrum (solid circles) and droplet nuclei spectra (open triangles) measured in three cloud regions on 2 August 1990 with droplet distributions shown in Fig. 9. Percent critical supersaturation is plotted on the abscissa and cumulative percent of total particle number on the ordinate. Distribution (a) was sampled at a CVI cut size of 10-μm diameter and had a median S_c of 0.05%. Distribution (b) was sampled at a CVI cut size of 19-μm diameter and had a median S_c of 0.04%. Distribution (c) was sampled at CVI cut size of 22-μm diameter and had a median S_c of 0.16%.

S_c's greater than 0.4% were incorporated into the droplets, despite the fact that only the large droplet "tail" of the spectrum was actually sampled.

Another cloud band located near shore on 10 August was studied extensively near cloud top, where low droplet concentrations were again observed. The six cloud-top regions sampled again had quite disparate $\bar{S}_c$'s, ranging from 0.01% to 0.27%, higher than for any of the ambient CCN spectra. This variation again could not be readily correlated to differences in the droplet size distribution and may indicate the influence of different types of mixing processes.

c. Discussion

The large variability in measured S_c spectra at cloud top was somewhat surprising. Since airflow motions can affect the relative wind with respect to the CVI inlet and potentially droplet collection efficiency, aircraft attitude and air motion data were also examined for a possible influence. No relationship between the median S_c's of the droplet nuclei and wind direction or aircraft attitude was found, however, indicating that changes in sampling angle were not the cause of the range of spectra observed.

A strong tendency for median S_c's to be lower for the droplet nuclei than for the ambient samples was observed, except at cloud top. Because the CVI usually sampled relatively large droplets within the cloud, this suggests that the larger droplets were more likely to contain low-S_c nuclei than the small droplets. One therefore might expect a relationship between CVI cut size and droplet nuclei $\bar{S}_c$, but even for samples from the same altitude, no clear relationship of this nature was detected. However, the number of samples was small. Also, because the droplet size distribution usually varied across the

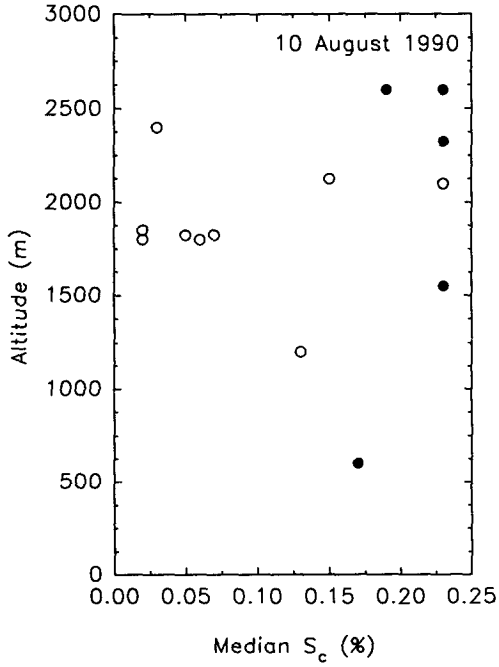

FIG. 11. As in Fig. 5 but for a rainband sampled at 1800–1901 10 August 1990.

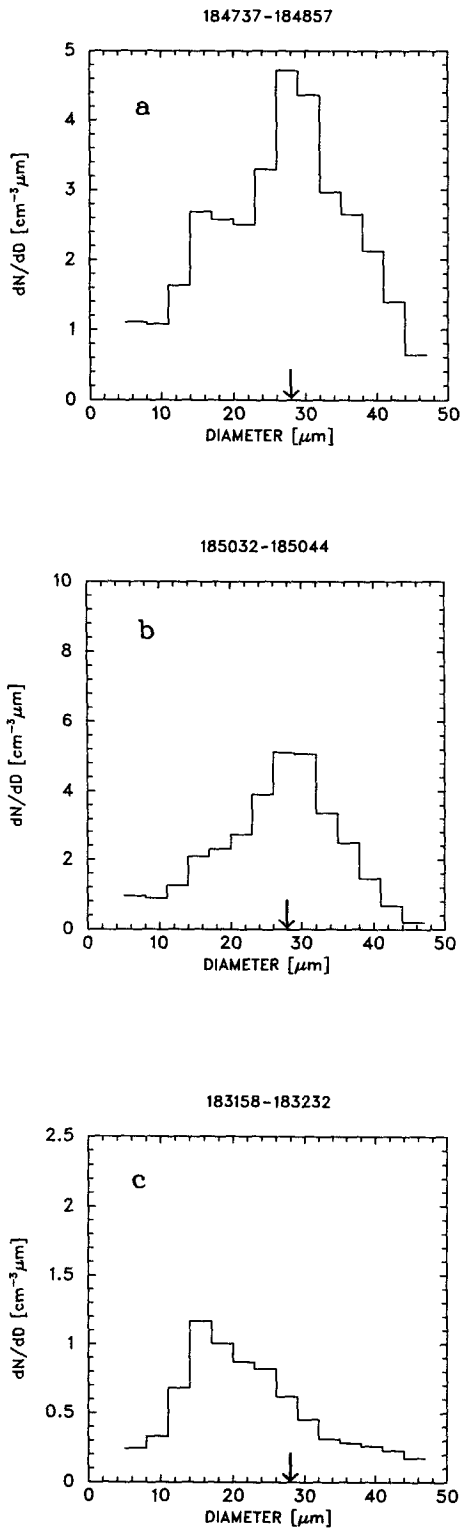

FIG. 12. Average droplet size distributions measured by the FSSP for three cloud regions sampled on 10 August 1990. Integrated number concentrations were 102 cm^{-3} for distribution (a) (1875-m altitude), 98 cm^{-3} for distribution (b) (1800 m), and 22 cm^{-3} for distribution (c) (2150 m). The minimum cut size used to sample each region with the CVI is indicated by an arrow on the abscissa of each plot.

rainband, each sample actually represented a cloud element with a unique thermodynamic history. As such, the properties of these disparate samples would not be expected to vary systematically with cut size. We do not believe that these results are necessarily indicative that mixing processes nullified the relationship between the droplet spectrum and the associated nucleus spectrum at the middle cloud levels, just that the sampled parcels had dissimilar histories. In this type of situation, a dual CVI that could be operated at two different cut sizes simultaneously would be needed to detect size-dependent variations in nuclei properties, if they were present.

An attempt was also made to construct mixing diagrams (Paluch 1979) in order to identify the origins of the air incorporated into a cloud. A number of difficulties, however, such as the well-mixed character of the boundary layer, the nonconservative nature of total water content (due to precipitation), and the wetting of sensors in cloud, prevented this approach.

Our results using this new technique in cumulus clouds show evidence of near-adiabatic growth near cloud base, with increasing involvement of entrainment and mixing at middle and upper cloud levels. The fact that significant differences between CVI-derived and ambient CCN spectra that are consistent with certain cloud processes were found demonstrates the fundamental merit of this experiment. The results presented here should be taken as preliminary, however, because of the limited quantitative nature of this analysis and the high degree of microphysical variability, particularly at the middle cloud levels, in these cumulus clouds. These limitations made it difficult to unequivocally distinguish inhomogeneous mixing from other types of mixing. Also, the below-cloud CCN spectra used for comparison purposes may not have been identical to the ones on which the sampled droplets were formed if, for example, the below-cloud spectrum had been recently modified by cloud processes, such as precipitation, or if some droplets had formed on different CCN entrained through the sides or top of the cloud. The presence of even high-S_c particles within relatively large droplets in some cloud-top regions, however, certainly suggests that inhomogeneous mixing (Baker et al. 1980) may in fact occur near cloud top in these vigorously entraining cumulus clouds.

This analysis served to suggest improvements for future investigations. For example, the time constant for the CCN spectrometer has since been decreased in order to capture smaller-scale structure, and the airborne CVI inlet is being redesigned to more efficiently transmit all droplet sizes. These improvements will permit more detailed and quantitative comparisons between the ambient and droplet nuclei spectra in the future.

4. Summary

To investigate relationships between the S_c spectra of ambient CCN and those of residual nuclei from

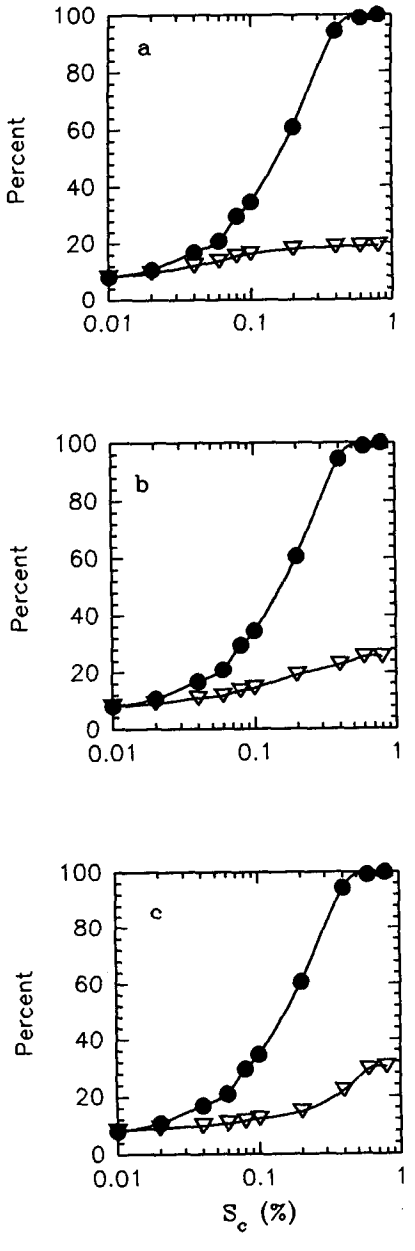

FIG. 13. Below-cloud CCN spectrum (solid circles) and droplet nuclei spectra (open triangles) measured in three cloud regions on 10 August 1990 with droplet distributions shown in Fig. 12. Percent critical supersaturation is plotted on the abscissa and cumulative percent of total particle number on the ordinate. Distribution (a) was sampled at a CVI cut size of 28-μm diameter and had a median S_c of 0.02%. Distribution (b) was sampled at a CVI cut size of 28-μm diameter and had a median S_c of 0.06%. Distribution (c) was sampled at CVI cut size of 28-μm diameter and had a median S_c of 0.23%.

droplets, the CVI was combined with a CCN spectrometer in a series of maritime cumuli cloud penetrations by aircraft. A compilation of median S_c's for nearly 100 cloud regions associated with 18 individual cumulus cloud bands showed that, in almost all cases, median S_c values were lower for the droplet nuclei than for the ambient CCN in the near-cloud environment. These results verify a general tendency for the lower-S_c nuclei to be preferentially incorporated into cloud droplets, despite evidence that entrainment and mixing occurred at most cloud levels.

The study also revealed interesting variations in the S_c spectra of droplet nuclei with height above cloud base. Regions near cloud base with near-adiabatic liquid water contents exhibited droplet nuclei spectra that were similar to those expected for adiabatic growth on measured below-cloud CCN spectra. Droplet nuclei in the middle regions of the cloud bands consistently exhibited median S_c's that were less than or equal to those that were measured in ambient air below and around the cloud, and particles with very high S_c's were still excluded from the larger droplets. The shapes of these spectra, however, were suggestive of some type of mixing process.

Nuclei spectra from droplets at or near cloud top displayed a wide variation in S_c characteristics. Spectra from some of the cloud-top regions seemed indicative of inhomogeneous mixing, with high-S_c particles present even within the larger cloud droplets. Further studies of this nature are being conducted with improved instrumentation to clarify the relationships between CCN and cloud microphysics in different cloud types, looking particularly at effects of mixing processes.

Acknowledgments. The authors wish to thank the staff of NCAR's Research Aviation Facility for excellent technical support during the Hawaiian Rainband Project. Special thanks are due to Tad Anderson, John Ogren, Al Cooper, and Greg Taylor for useful suggestions and to Bob Charlson for encouraging the transfer of the CVI technology to NCAR. Tad Anderson at the University of Washington calculated droplet transmission efficiency inside the CVI. The NCAR Advanced Studies Program, as well as NASA through Cooperative Agreement ATM-9209181, provided funding for C. Twohy. J. Hudson was supported by ONR N00014-91-J-1090 and NSF ATM 8919935.

APPENDIX

CVI Sampling Characteristics

The CVI operates on the principle of inertial impaction, where droplets (or ice particles) having sufficient inertia are impacted into a slowly moving flow of dried, filtered air. The relative wind due to the aircraft motion provides the impaction velocity for the airborne CVI. For droplets with sufficient inertia to enter the CVI against the counterflow airstream, the number of droplets entering during a time period t equals the number concentration $N_{d,o}$ of these droplets that are outside the probe times the air flow rate impinging on the CVI probe tip. This droplet number also equals the number concentration of droplets inside the CVI $N_{d,i}$ times the air volume inside the CVI; hence,

$$N_{d,o}AV_ot = N_{d,i}AV_it,$$

where A is the cross-sectional open area of the inlet tip, V_o is the droplet speed as it approaches the inlet tip, and V_i is the droplet speed inside the inlet. The ratio of droplet number concentration inside the CVI to that in the ambient airstream may then be described as

$$\frac{N_{d,i}}{N_{d,o}} = \frac{V_o}{V_i}.$$

The droplet speed V_o may be approximated by the aircraft true airspeed and V_i by the mean flow speed inside the CVI; for typical values of 120 and 5 m s^{-1}, droplet concentrations inside the CVI are enhanced by a factor of 24. The initial enhancement of droplets inside the CVI means that substantial concentrations of droplet nuclei will still be collected, even if transmission efficiency of these droplets through the inlet system is less than 100% (see below).

Some cloud droplets that enter the airborne CVI inlet will be deposited on internal surfaces, either by gravitational settling or by direct impaction, before they completely evaporate. Both model calculations (T. L. Anderson 1994, personal communication) and measurements (Twohy 1992b) indicate that the transmission efficiency for droplet nuclei averages about 50%. However, efficiency can vary with probe alignment, flow rate, and droplet size. To minimize losses due to misalignment, the CVI axis was aligned with the mean flow streamlines predicted by airflow analysis (Twohy and Rogers 1993).

Additional modeling and comparisons of model results to measurements is under way to better characterize transmission efficiency under different conditions. Corrections to measured droplet nuclei concentrations could be made either by using model results or by scaling to the droplet concentrations measured by the FSSP in different size ranges. However, due to the large uncertainty in model results and FSSP measurements (Baumgardner et al. 1990), we have not chosen either of these approaches. Instead, we simply present droplet nuclei characteristics in terms of median S_c's or as normalized S_c spectra, which should not be influenced by errors in absolute number concentrations. Variations in efficiency as a function of droplet size could, however, influence the shape of the S_c spectra. Calculations indicate that transmission efficiency is a slowly varying function of droplet size and is maximized just above the minimum cut size (T. L. Anderson 1994, personal communication). When possible, the internal flow rate and the cut size of the probe were adjusted to maximize enhancement and transmission efficiency for droplets of interest. For example, when the droplet size distribution peaked at relatively large droplet sizes (20–30 μm), the sample flow rate inside the CVI inlet might be decreased, increasing the counterflow rate and the minimum droplet cut size. The reduced internal flow rate minimizes impaction losses of larger droplets in the bend immediately downstream of the inlet. (Nuclei from droplets approximately 40 μm and larger in diameter will not be transmitted by this version of the CVI because they will impact in the bend before they evaporate to sizes small enough to be transmitted. Fortunately, the number concentrations of these droplets were only a few percent or less of the total droplet concentration and should not affect our results.)

We have undertaken detailed analyses of droplet nuclei spectra primarily for those sampling situations where these size-dependent transmission effects should be small (e.g., relatively narrow droplet distributions and those with maximum concentrations near the CVI cut size). We have also considered the possible influence of size-dependent losses in the discussion of our results.

The frequent presence of drizzle and precipitation-sized droplets in the Hawaiian clouds led to another complication. If these very large droplets had sufficient kinetic energy upon impaction to break up, enhanced particle concentrations were observed downstream of the inlet when the resulting smaller droplets evaporated. Trajectory calculations predict that the position of the CVI during HaRP was actually shielded from drops 100 to 800 μm in diameter by the aircraft itself (Twohy and Rogers 1993). Also, comparisons of particle concentrations downstream of the CVI inlet with large drop concentrations measured by PMS 2D probes indicated that drops larger than 800 μm were the most likely to breakup and generate enhanced particle concentrations. This breakup phenomenon, discussed in more detail by Twohy (1992b), has also apparently been observed using more standard inlets for sampling particles in clouds (Hudson and Frisbie 1991; Hudson 1993b).

Time periods when drop breakup was judged to occur were eliminated from the dataset. CVI particle concentrations were compared to droplet concentrations measured by the FSSP, and data from any time period when the droplet nuclei concentration inside the CVI was greater than twice that expected from the FSSP data were discarded. This approach was justified when several of these rejected time periods were examined and drops larger than 800 μm were found to be present; conversely, a survey of several time periods that were retained verified that drops larger than 800 μm were not present.

REFERENCES

Albrecht, B. A., 1989: Aerosols, cloud microphysics, and fractional cloudiness. *Science*, **245**, 1227–1230.

Arking, A., 1991: The radiative effects of clouds and their impact on climate. *Bull. Amer. Meteor. Soc.*, **72**, 795–813.

Baker, M. B., and J. Latham, 1992: A quasi-analytic model of droplet and CCN lifetimes, optical and chemical characteristics of ice-free cumulus clouds. *Quart. J. Roy. Meteor. Soc.*, **118**, 851–875.

——, R. G. Corbin, and J. Latham, 1980: The influence of entrainment on the evolution of cloud droplet spectra: I. A model of inhomogeneous mixing. *Quart. J. Roy. Meteor. Soc.*, **106,** 581–598.

Baumgardner, D., and M. Spowart, 1990: Evaluation of the forward scattering spectrometer probe. Part III: Time response and laser inhomogeneity limitations. *J. Atmos. Oceanic Technol.*, **7,** 666–672.

——, W. A. Cooper, and J. E. Dye, 1990: Optical and electronic limitations of the forward-scattering spectrometer probe. *Liquid Particle Size Measurement Techniques:* Vol. 2, E. Dan Hirleman et al., Eds., Amer. Soc. Test. Mater., 115–127.

Beard, K. V., and H. T. Ochs, 1993: Warm-rain initiation: An overview of microphysical mechanisms. *J. Appl. Meteor.*, **32,** 608–625.

Blyth, A. M., W. A. Cooper, and J. B. Jensen, 1988: A study of the source of entrained air in Montana cumuli. *J. Atmos. Sci.*, **45,** 3944–3964.

Bower, K. N., and T. W. Choularton, 1992: An investigation of the processes controlling the liquid phase microphysics of stratocumulus and cumulus clouds. *Proc. 11th Int. Conf. on Clouds and Precipitation,* Montreal, Quebec, Canada, Int. Assoc. Meteor. and Atmos. Phys., 122–124.

——, and ——, 1993: Cloud processing of the cloud condensation nucleus spectrum and its climatological consequences. *Quart. J. Roy. Meteor. Soc.*, **119,** 655–679.

Charlson, R. J., S. E. Schwartz, J. M. Hales, R. D. Cess, J. A. Coakley Jr., J. E. Hansen, and D. J. Hofmann, 1992: Climate forcing by anthropogenic aerosols. *Science,* **255,** 423–430.

Cheng, Y.-S., and C.-S. Wang, 1975: Inertial deposition of particles in a bend. *Aerosol Sci.*, **6,** 139–145.

Clarke, A. D., N. C. Alquist, and D. S. Covert, 1987: The Pacific marine aerosol: Evidence for natural acid sulfates. *J. Geophys. Res.*, **92,** 4179–4190.

Cooper, W. A., 1989: Effects of variable droplet growth histories on droplet size distributions. Part I: Theory. *J. Atmos. Sci.*, **46,** 1301–1311.

Easter, R. C., and P. V. Hobbs, 1974: The formation of sulfates and the enhancement of cloud condensation nuclei in clouds. *J. Atmos. Sci.*, **31,** 1586–1594.

Fitzgerald, J. W., and P. A. Spyers-Duran, 1973: Changes in cloud nucleus concentration and cloud droplet size distribution associated with pollution from St. Louis. *J. Appl. Meteor.*, **12,** 511–515.

Fletcher, N. H., 1969: *The Physics of Rainclouds.* Cambridge University Press, 390 pp.

Flossmann, A. I., 1991: The scavenging of two different types of marine aerosol particles calculated using a two-dimensional detailed cloud model. *Tellus,* **43B,** 301–321.

——, W. D. Hall, and H. R. Pruppacher, 1985: A theoretical study of the wet removal of atmospheric pollutants. Part I: The redistribution of aerosol particles captured through nucleation and impaction scavenging by growing cloud drops. *J. Atmos. Sci.*, **42,** 583–606.

Frisbie, P. R., and J. G. Hudson, 1993: Urban cloud condensation nuclei spectral flux. *J. Appl. Meteor.*, **32,** 666–676.

Gerber, H., 1991: Supersaturation and droplet spectral evolution in fog. *J. Atmos. Sci.*, **48,** 2569–2588.

Hegg, D. A., and P. V. Hobbs, 1979: The homogenous oxidation of sulfur dioxide in cloud droplets. *Atmos. Environ.*, **13,** 981–987.

——, and T. V. Larson, 1990: The effects of microphysical parameterization on model predictions of sulfate production in clouds. *Tellus,* **42B,** 272–284.

——, L. F. Radke, and P. V. Hobbs, 1991: Measurements of Aitken nuclei and cloud condensation nuclei in the marine atmosphere and their relation to the DMS-cloud-climate hypothesis. *J. Geophys. Res.*, **96,** 18 727–18 733.

Heintzenberg, J. A., J. A. Ogren, K. J. Noone, and L. Gardneus, 1989: The size distribution of submicrometer particles within and about stratocumulus cloud droplets on Mt. Areskutan, Sweden. *Atmos. Res.*, **24,** 89–101.

Herrera, J. R., and J. J. Castro, 1988: Production of cloud condensation nuclei in Mexico City. *J. Appl. Meteor.*, **27,** 1189–1192.

Hindman, E. E., W. M. Porch, J. G. Hudson, and P. A. Durkee, 1994: Ship-produced cloud lines of 13 July 1991. *Atmos. Environ.*, **28,** 3393–3403.

Hocking, L. M., 1959: The collision efficiency of small drops. *Quart. J. Roy. Meteor. Soc.*, **85,** 44–50.

Hoppel, W. A., J. W. Fitzgerald, G. M. Frick, and R. E. Larson, 1990: Aerosol size distribution and optical properties found in the marine boundary layer over the Atlantic Ocean. *J. Geophys. Res.*, **95,** 3659–3686.

Howell, W. E., 1949: The growth of cloud drops in uniformly cooled air. *J. Meteor.*, **6,** 134–148.

Hudson, J. G., 1982: Correlation between surface and cloud base CCN spectra in Montana. *J. Appl. Meteor.*, **21,** 1427–1440.

——, 1983: Effect of CCN concentrations on stratus clouds. *J. Atmos. Sci.*, **40,** 480–486.

——, 1984: Cloud condensation nuclei measurements within clouds. *J. Climate Appl. Meteor.*, **23,** 42–51.

——, 1989: An instantaneous CCN spectrometer. *J. Atmos. Oceanic Technol.*, **6,** 1055–1065.

——, 1991: Observations of anthropogenic CCN. *Atmos. Environ.*, **25A,** 2449–2455.

——, 1993a: Cloud condensation nuclei. *J. Appl. Meteor.*, **32,** 596–607.

——, 1993b: Cloud condensation nuclei near marine cumulus. *J. Geophys. Res.*, **98,** 2693–2702.

——, and C. Rogers, 1986: Relationship between critical supersaturation and cloud droplet size: Implications for cloud mixing processes. *J. Atmos. Sci.*, **43,** 2341–2359.

——, and P. R. Frisbie, 1991: Cloud condensation nuclei near marine stratus. *J. Geophys. Res.*, **96,** 20 795–20 808.

——, and A. D. Clarke, 1992: Aerosol and cloud condensation nuclei measurements in the Kuwait plume. *J. Geophys. Res.*, **97,** 14 533–14 536.

Huebert, B. J., and A. L. Lazrus, 1980: Bulk composition of aerosols in the remote troposphere. *J. Geophys. Res.*, **85,** 7337–7344.

Jensen, J. B., and M. B. Baker, 1989: A simple model of droplet spectral evolution during turbulent mixing. *J. Atmos. Sci.*, **46,** 2812–2829.

——, P. H. Austin, M. B. Baker, and A. M. Blyth, 1985: Turbulent mixing, spectral evolution and dynamics in a warm cumulus cloud. *J. Atmos. Sci.*, **42,** 173–192.

Jiusto, J. E., 1966: Maritime concentration of condensation nuclei. *J. Rech. Atmos.*, **2,** 245–250.

Kaufman, Y. J., R. S. Fraser, and R. L. Mahoney, 1991: Fossil fuel and biomass burning effect on climate—Heating or cooling? *J. Climate,* **4,** 578–588.

Leaitch, W. R., J. W. Strapp, G. A. Isaac, and J. G. Hudson, 1986: Cloud droplet nucleation and scavenging of aerosol sulphate in polluted atmospheres. *Tellus,* **388,** 328–344.

Lee, I. Y., G. Hanel, and H. R. Pruppacher, 1980: A numerical determination of the evolution of cloud drop spectra due to condensation on natural aerosol particles. *J. Atmos. Sci.*, **37,** 1839–1853.

Liou, K. N., and S. C. Ou, 1989: The role of cloud microphysical processes in climate: An assessment from a one dimensional perspective. *J. Geophys. Res.*, **94,** 8599–8607.

Mason, B. J., 1971: *The Physics of Clouds.* Oxford University Press, 671 pp.

——, and P. Jonas, 1974: The evolution of droplet spectra and large droplets by condensation in cumulus clouds. *Quart. J. Roy. Meteor. Soc.*, **100,** 23–28.

Noone, K. J., R. J. Charlson, D. S. Covert, J. A. Ogren, and J. Heintzenberg, 1988a: Cloud droplets: Solute concentration is size-dependent. *J. Geophys. Res.*, **93D,** 9477–9482.

——, ——, ——, ——, and ——, 1988b: Design and calibration of a counterflow virtual impactor for sampling of atmospheric fog and cloud droplets. *Aerosol Sci. Technol.*, **8,** 235–244.

Ogren, J. A., and R. J. Charlson, 1992: Implications for models and measurements of chemical inhomogeneities among cloud droplets. *Tellus,* **44B,** 208–225.

——, J. Heintzenberg, and R. J. Charlson, 1985: In-situ sampling of clouds with a droplet to aerosol converter. *Geophys. Res. Lett.,* **12,** 121–124.

——, ——, A. Zuber, K. J. Noone, and R. J. Charlson, 1989: Measurements of the size-dependence of solute concentrations in cloud droplets. *Tellus,* **41B,** 24–31.

——, K. J. Noone, A. Hallberg, J. Heintzenberg, D. Schell, A. Berner, I. Solly, C. Kruisz, G. Reischl, B. G. Arends, and W. Wobrock, 1992: Measurements of the size dependence of the concentrations of non-volatile material in cloud droplets. *Tellus,* **44B,** 570–580.

Paluch, I. R., 1979: The entrainment mechanism in Colorado cumuli. *J. Atmos. Sci.,* **36,** 2467–2478.

Parungo, F., C. Nagomoto, I. Nolt, M. Dias, and E. Nickerson, 1982: Chemical analysis of cloud water collected over Hawaii. *J. Geophys. Res.,* **87,** 8805–8810.

Pruppacher, H. R., and J. D. Klett, 1978: *Microphysics of Clouds and Precipitation.* D. Reidel, 714 pp.

Radke, L. F., and P. V. Hobbs, 1969: Measurement of cloud condensation nuclei, light-scattering coefficient, sodium-containing particles, and Aitken nuclei in the Olympic Mountains of Washington. *J. Atmos. Sci.,* **26,** 281–288.

Raga, G. B., J. B. Jensen, and M. B. Baker, 1990: Characteristics of cumulus bands off the coast of Hawaii. *J. Atmos. Sci.,* **44,** 2150–2165.

Roelofs, G. J. H., 1992: Drop size dependent sulfate distribution in a growing cloud. *J. Atmos. Chem.,* **14,** 109–118.

Squires, P., 1952: The growth of cloud drops by condensation. *Aust. J. Sci. Res.,* **A5,** 59–86.

——, 1966: An estimate of the anthropogenic production of cloud nuclei. *J. Rech. Atmos.,* **2,** 297–307.

——, 1972: Diffusion chambers for the measurement of cloud nuclei. *J. Rech. Atmos.,* **6,** 565–572.

Telford, J. W., and S. K. Chai, 1980: A new aspect of condensation theory. *Pure Appl. Geophys.,* **118,** 720–742.

Twohy, C. H., 1992a: Sampling artifacts produced in aircraft aerosol inlets by the presence of large cloud droplets. *Abstracts, 11th Annual Meeting,* San Francisco, CA, Amer. Assoc. for Aerosol Res., p. 300.

——, 1992b: On the size dependence of the chemical properties of cloud droplets: Exploratory studies by aircraft. Ph.D. dissertation, University of Washington, 239 pp. [NCAR Cooperative Thesis No. 137.]

——, and D. Rogers, 1993: Airflow and water-drop trajectories at instrument sampling points around the Beechcraft King Air and Lockheed Electra. *J. Atmos. Oceanic Technol.,* **10,** 1993.

——, P. A. Austin, and R. J. Charlson, 1989: Chemical consequences of the initial diffusional growth of cloud droplets: A clean marine case. *Tellus,* **41B,** 51–60.

Twomey, S., 1977a: The influence of pollution on the shortwave albedo of clouds. *J. Atmos. Sci.,* **34,** 149–152.

——, 1977b: *Atmospheric Aerosols.* Elsevier, 302 pp.

——, and P. Squires, 1959: The influence of cloud nucleus population on the microstructure and stability of convective clouds. *Tellus,* **11,** 408–411.

——, and J. Warner, 1967: Comparison of measurements of cloud droplets and cloud nuclei. *J. Atmos. Sci.,* **24,** 702–703.

Walcek, C. J., and G. R. Taylor, 1986: A theoretical method for computing vertical distributions of acidity and sulfate production within cumulus clouds. *J. Atmos. Sci.,* **43,** 339–355.

Warner, J., 1969: The microstructure of cumulus cloud. Part II: The effect on droplet size distribution of the cloud nucleus spectrum and updraft velocity. *J. Atmos. Sci.,* **26,** 1272–1282.

Wigley, T. M. L., 1991: Could reducing fossil-fuel emissions cause global warming? *Nature,* **349,** 503–506.